Conference Paper, Published Version

Liang, Dongfang; Cheng, Liang; Yeow, Kervin

Numerical Modelling of Current Induced Scour under Offshore Pipelines

NUMERICAL MODELLING OF CURRENT INDUCED SCOUR UNDER OFFSHORE PIPELINES

DONGFANG LIANG , LIANG CHENG AND KERVIN YEOW

School of Civil and Resource Engineering, The University of Western Australia
35 Stirling Highway, Crawley, WA6009, Australia

Local scour evolutions under a pipeline are simulated using a vertical two-dimensional numerical model. The pipe is originally residing on or above a flat sand bed and subject to steady currents. The numerical model computes the developments of the flow and sediment transport with the update of the bed-shape based on the mass balance of sediment. Governing equations are solved by finite difference method in a non-orthogonal boundary-fitted curvilinear coordinate system. The Wilcox k-ω model is used as the turbulence closure. Both suspended and bed loads of sediment are considered in the model. The computational grid is adapted to the new geometry by solving a Poisson equation after each bed update. A sand slide model is employed in the simulation of the morphological change. Different time steps are used to march the flow and bed-profile in the model to reduce the computational cost. Scour predictions are compared with independent laboratory measurements. The vortex shedding phenomenon is captured at a later stage of the scour development and the predicted scour profiles agree well with those measured independently.

1 Introduction

Pipelines on erodible beds are subject to local scour due to the dynamic interactions among pipelines, flow and sediment transport. After the scour happens, the unsupported pipeline is often very vulnerable to damages. The consequence of the pipeline failure is severe both economically and environmentally. Most of the previous investigations on the local scour around pipelines are through physical modeling, from which many empirical formulas on the scour depth were proposed.

Considerable progress has been made in the development of numerical models for local scour around pipelines. Over the last three decades, some numerical models for scour prediction have been proposed. Some are based on the potential flow theory, such as Chao & Hennessy (1972), Hansen *et al*. (1986), Chiew (1991), and Li and Cheng (1999). The other are based on viscous/turbulent flow models, such as Leeuwenstein *et al*. (1985), Sumer *et al*. (1988), van Beek and Wind (1990), Brørs (1999), Li and Cheng (2000 & 2001) and Liang *et al*. (2004). The turbulent flow approach is more appropriate because the separation and vortex movement cannot be described by the potential flow theory. Cheng (2002) presented a detailed review on this topic.

However, it is not an easy task to predict the development of the scour process correctly. The model proposed by Brørs (1999) was claimed to include both suspended and bed loads. It is noted that the threshold Shields parameter for sediment suspension was set as 0.25 in that model which is much larger than the undisturbed Shields parameter (0.048) in the following pipeline-scour simulation, so it is suspected that the suspended load in the model of Brørs (1999) does not take any effect. On the contrary,

the model by Li and Cheng (2000) included suspended load only. It seems that there is still room for further development as far as numerical modeling of scour is concerned.

In order to model the scour process well, both accurate flow model and proper sediment transport model are needed. This paper develops a numerical model that is capable of predicting the time development of the local scour around a pipeline. Some key techniques, such as the time marching scheme and sand slide model, are introduced first. Then the scour evolutions are calculated for the situations of the undisturbed Shields parameter θ_∞=0.098 and initial gap ratios e/D=0 and 0.5, where e is the gap between the pipe and the undisturbed sand bed and D is the pipe diameter. The predicted results agree reasonably well with the experimental data not only in the equilibrium scour depth but also in the whole time development process of the scour hole.

2 Mathematical Formulation

2.1 Governing Equations

The two-dimensional ensemble-averaged continuity and Navier-Stokes equations with k-ω turbulence closure are used to simulate the flow field, which can be written in the following dimensionless form.

$$\frac{\partial u}{\partial x}+\frac{\partial v}{\partial y}=0 \tag{1}$$

$$\frac{\partial u}{\partial t}+u\frac{\partial u}{\partial x}+v\frac{\partial u}{\partial y}=-\frac{\partial p}{\partial x}+\frac{1}{\mathrm{Re}}\left(\frac{\partial^2 u}{\partial x^2}+\frac{\partial^2 u}{\partial y^2}\right)+\frac{\partial \tau_{xx}}{\partial x}+\frac{\partial \tau_{xy}}{\partial y} \tag{2}$$

$$\frac{\partial v}{\partial t}+u\frac{\partial v}{\partial x}+v\frac{\partial v}{\partial y}=-\frac{\partial p}{\partial y}+\frac{1}{\mathrm{Re}}\left(\frac{\partial^2 v}{\partial x^2}+\frac{\partial^2 v}{\partial y^2}\right)+\frac{\partial \tau_{xy}}{\partial x}+\frac{\partial \tau_{yy}}{\partial y} \tag{3}$$

$$\frac{\partial k}{\partial t}+u\frac{\partial k}{\partial x}+v\frac{\partial k}{\partial y}=\frac{1}{\mathrm{Re}}\left(\frac{\partial^2 k}{\partial x^2}+\frac{\partial^2 k}{\partial y^2}\right)+\frac{\partial}{\partial x}\left(\frac{\nu_t}{\sigma_{k1}}\frac{\partial k}{\partial x}\right)+\frac{\partial}{\partial y}\left(\frac{\nu_t}{\sigma_{k1}}\frac{\partial k}{\partial y}\right)+P_k-\beta^*\omega k \tag{4}$$

$$\frac{\partial \omega}{\partial t}+u\frac{\partial \omega}{\partial x}+v\frac{\partial \omega}{\partial y}=\frac{1}{\mathrm{Re}}\left(\frac{\partial^2 \omega}{\partial x^2}+\frac{\partial^2 \omega}{\partial y^2}\right)+\frac{\partial}{\partial x}\left(\frac{\nu_t}{\sigma_{\omega 1}}\frac{\partial \omega}{\partial x}\right)+\frac{\partial}{\partial y}\left(\frac{\nu_t}{\sigma_{\omega 1}}\frac{\partial \omega}{\partial y}\right)+\frac{\gamma_1}{\nu_t}P_k-\beta_1\omega^2 \tag{5}$$

where u and v are the horizontal (x) and vertical (y) velocity components respectively; p is pressure; t is time; Re is the Reynolds number; τ is the turbulent shear stress; k is the turbulent kinetic energy, ω is the specific dissipation rate of k; P_k is the production rate of k by the mean velocity shear; $\upsilon_t = \alpha^* k/\omega$ is the turbulent viscosity; σ_{k1}, $\sigma_{\omega 1}$, β^*, β_1, γ_1 and α^* are the k-ω model coefficients (Wilcox, 1994).

A distinction is made between the bed load and suspended load in the sediment transport model. In this research, the bed load transport formula proposed by van Rijn (1987) is adopted.

$$q_b = \begin{cases} 0.053[(s-1)g]^{0.5} \dfrac{d_{50}^{1.5} T^{2.1}}{D_*^{0.3}} & , \quad T > 0 \\ 0 & , \quad T \le 0 \end{cases} \tag{6}$$

where $T = (u_*^2 - u_{*c}^2)/u_{*c}^2$ is the transport stage parameter; u_* and u_{*c} are the bed friction velocity and the critical friction velocity for sediment initiation respectively; s is the sediment specific weight; g is the gravity acceleration; d_{50} is the median sediment diameter; and D_* is the nondimensional sediment size defined as $D^* = [g(s\text{-}1)/v^2]^{1/3} d_{50}$. It should be noted that u_{*c} should be calculated by modifying the critical friction velocity for sediment motion on a flat bed so that the effect of bed slope is taken into account.

The suspended sediment concentration c is governed by the following transport equation.

$$\frac{\partial c}{\partial t} + u\frac{\partial c}{\partial x} + (v - \omega_s)\frac{\partial c}{\partial y} = \frac{\partial}{\partial x}\left(\frac{\nu_t}{\sigma_c}\frac{\partial c}{\partial x}\right) + \frac{\partial}{\partial y}\left(\frac{\nu_t}{\sigma_c}\frac{\partial c}{\partial y}\right) \tag{7}$$

where σ_c is taken to be 0.8 and ω_s is the sediment falling velocity.

The bed elevation is calculated based on the mass balance of the sediment material.

$$(1-n)\frac{\partial y_b}{\partial t} + \frac{\partial (q_b + \int cu \cdot dy)}{\partial x} = 0 \tag{8}$$

where n is the porosity of the sand bed and the integration is along the whole water column.

2.2 Computational Domain and Boundary Conditions

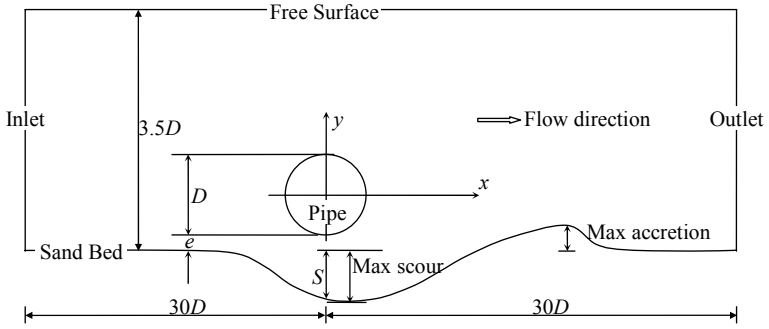

Figure 1. Sketch map of the computational domain and boundary types.

The computational domain and the boundaries are illustrated in Fig. 1. At the inlet, the fully-developed turbulent boundary layer flow is specified and the sediment concentration is given by Rouse profile. At the outlet, the natural boundary condition is used. The free surface is treated as a rigid lid and smooth-wall-function boundary condition is employed on the pipe surface, and no-flux boundary condition is employed

for the sediment concentration in these two boundaries. Rough-wall-function boundary condition is specified at the sand bed and the reference sediment concentration is solved from the empirical formula of van Rijn (1987).

3 Numerical Methods

3.1 Differential Equation Solver

Governing equations are solved using the finite difference method in a general curvilinear coordinate system. The pressure and velocity are coupled by a derived pressure Poisson equation. For details of the numerical implementation, readers are referred to Lei *et al*. (1999).

3.2 Sand Slide Model

Because of the complicated behavior of the sediment transport phenomenon and its nonlinear interaction with the flow field, positive feed back often occurs in the bed elevation update which can then lead to unrealistic morphologies of the bed and numerical instability. It was found that the numerical instabilities often occur when the predicted slope of the scour hole exceeds the angle of repose of the sediment. A sand slide model is introduced in this study after each sand bed update. Essentially it is a kind of smoothing technique which filters out the small irregularities on the bed. Care is taken that the bed shape is modified only where the scour slope exceeds the angle of repose of the sediment, so that the numerical diffusion introduced into the computation is very limited. Liang *et al.* (2004) discussed this technique in details. Fig. 2 shows the snapshots of the computational mesh using same computational parameters, but one without and one with the sand slide model in the computation. It is seen that this sand slide model only removes the unrealistic sharpness while most part of the bed remains unchanged.

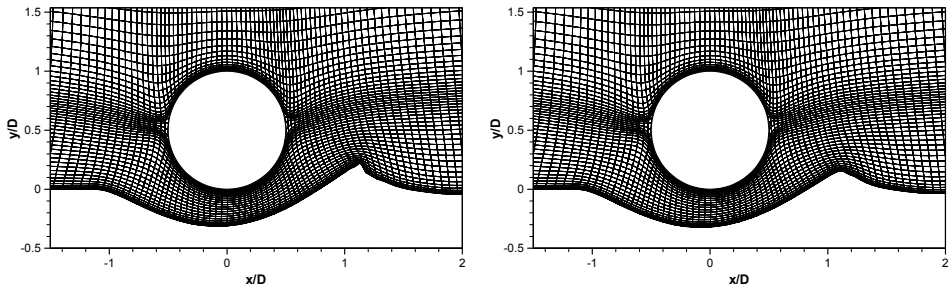

Figure 2. Corresponding bed shapes without (left) and with (right) the sand slide model, θ_∞=0.065, t=1.94 min.

3.3 Time Marching Scheme

The flow field change and the morphological change due to scouring have different time

scales. The flow field changes much faster than the sand bed morphological change. These fast-changing and slowly-changing processes need to be incorporated together. To achieve this, a time marching scheme as illustrated in Fig. 3 is adopted in this study. First of all, different time steps for the flow computation and morphological computation are used. It is possible to speed up the calculations by using a larger morphological time step Δt_{morph}, where $\Delta t_{morph} > \Delta t_{flow}$. Secondly, only a limited number of time steps of the flow field calculation are carried out after each morphological update and then the latest flow field is used as the representative flow field in predicting the subsequent scour profile.

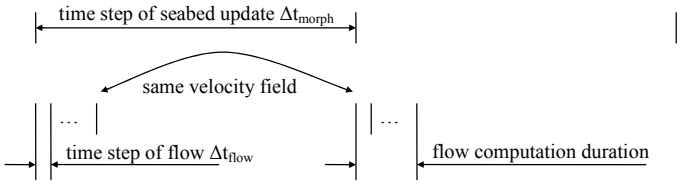

Figure 3. Illustration of the time marching schemes that combines the flow and scour calculations.

There are basically two methods to determine the morphological time step Δt_{morph}. One is to simply specify a fixed Δt_{morph} in the whole computation. This is not a good approach as can be seen in Fig. 4. The scour depth reaches its equilibrium value roughly in an exponential manner. Small Δt_{morph} has to be adopted to capture the rapid change of the scour depth at the beginning, which seems not necessary at final stage when the scour hole development is close to equilibrium. The other method, which is used in this study, is to determine Δt_{morph} by specifying the maximum deformation along the bed in each morphological update. In this way, Δt_{morph} is determined adaptively based on the scour rate. The morphological time step determined this way is small at the early stage and large at the final stage of the scour process.

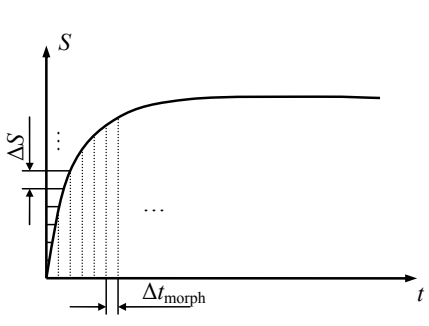

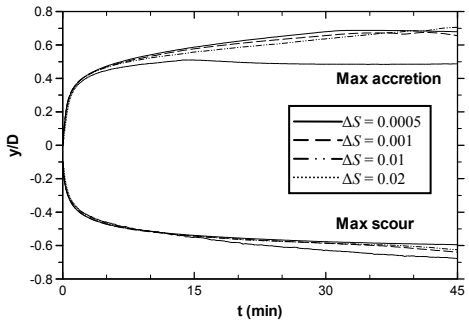

Figure 4. (Left figure) Different methods to determine the morphological time step.

Figure 5. (Right figure) The dependence of the prediction results on ΔS, θ_∞=0.065.

Between two consecutive bed updates, the flow model is run for a number of time

steps to allow the far-field flow to travel 0.1 D. The period of time that is covered in the flow computation, $0.1D/U$ (U is the depth averaged velocity), is still much smaller than the morphological time step Δt_{morph}, so that the present time marching scheme is able to accelerate the computation significantly. Different values of the maximum allowed bed deformation, ΔS, are examined in this study. The results indicate that the scour calculation is relatively independent on this value as seen from Fig. 5, where the maximum scour and accretion increments in each morphological time step are examined as a function of the maximum allowable bed deformation ΔS. In the following computation, $\Delta S = 0.001$ is used.

4 Results

4.1 Flow and Sediment Transport Fields

The two snapshots in Fig. 6 show the flow and sediment concentration fields at the tunnel and lee-wake scour stages respectively. In the figure, the shaded contours near the scoured seabed represent the concentration of sediment. During the early stage of the scour development, substantial amount of sand is rushed out of the bed underneath the pipe with a strong flow jet in the gap between the pipe and the bed. The sand is deposited just behind the pipe forming a steep sand ridge. The shear stress amplification in the narrow gap below the pipe is the major cause of violent tunnel erosion. Tunnel erosion normally takes place in a very short period of time and is responsible for the major expansion of the scour hole underneath the pipe. It is seen from the figure that there is a high concentration area immediately behind the pipe and it moves downstream gradually as the scour hole develops. As the gap between the pipeline and the bed is enlarged and the sand ridge is smoothed and moved downstream, tunnel scour gives its way to the lee-wake scour. The lee-wake scour generally has a much larger time scale than the tunnel scour. The vortex shedding is formed and the downstream scour slope becomes quite gentle. In the equilibrium state, the bottom shear stress near the pipeline almost approaches the shear stress of the incoming flow so that the sediment transport rate is about the same at every point on the bed. This is manifested in the figure that the sediment concentration at the bottom becomes small and almost evenly distributed along the bed. Due to the presence of slope in the bed, shear stress does not necessarily need to be exactly the same everywhere.

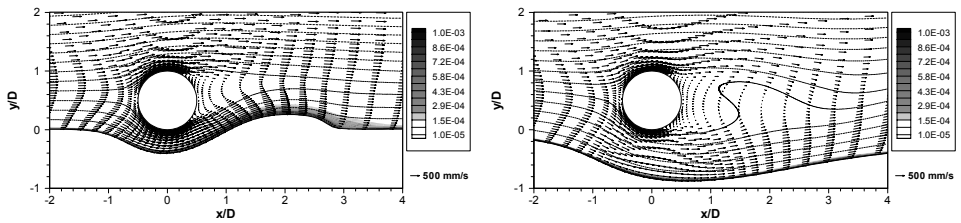

Figure 6. Snapshots of the computed flow and sediment concentration fields at 1 min and 90 min, θ_∞=0.098.

4.2 Scour Profile

The calculated development of scour shapes are compared with measured ones in Figs. 7. The experiment was reported in Fig. 2.22 of Mao (1986). Generally speaking, the predicted scour profile under the pipeline agrees well with the experimental results. An interesting phenomenon is observed that as the pipe is moved 0.5 D away from the original flat bed the scour shows no sign to abate, instead the scour depth remains almost unchanged. Whereas, the location of the deepest scour moves downstream and hence the scour width becomes larger in the case of e/D=0.5.

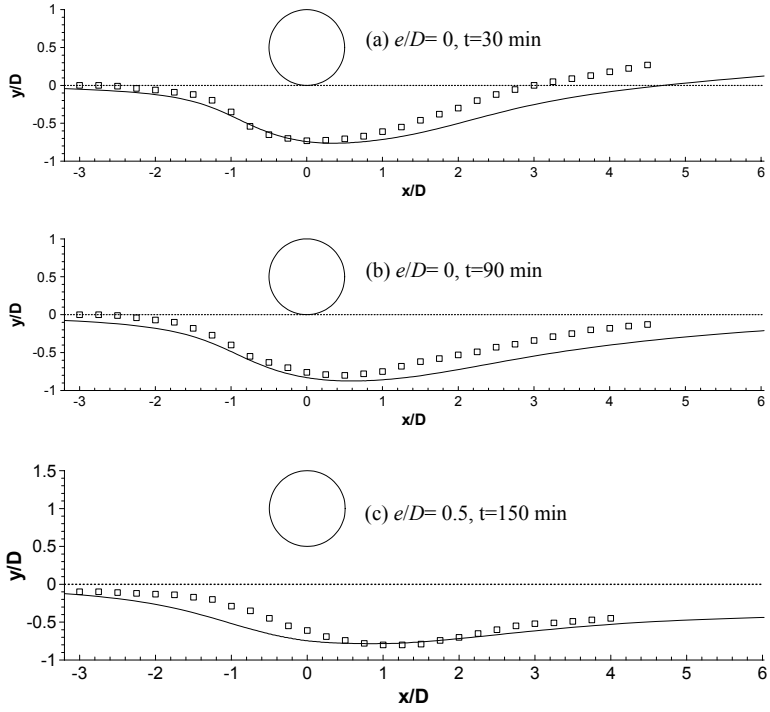

Figure 7. The comparison of the computed (solid line) scour profile with the experiment data (hollow box), θ_∞=0.098.

5 Conclusions

A vertical 2D numerical model has been developed to predict the scour process under pipelines. Both bed load and suspended load of sediment transport are accounted in the model. The bed deformation is based on the sediment mass balance equation integrated over the water depth. The differential equations are solved by finite difference method in a body-fitted coordinate system. A sand slide model is introduced to smooth the bed

deformation. Due to the different time scales of the flow and morphological change, different time steps are employed in flow field and bed geometry computations. The integrated model is used to predict the scour development under the pipeline. The well-organized vortex shedding is observed at the final stage of the calculation. The computed results compare well with the experimental data.

Acknowledgments

The authors would like to acknowledge the support from the Australia Research Council through ARC Discovery Projects Program Grant No. DP0210660. This work is carried out while the first author is an academic visitor at School of Civil and Resource Engineering, The University of Western Australia.

References

Brørs, B. (1999). "Numerical modeling of flow and scour at pipelines." *J. Hydr. Engrg.*, 125(5), 511-523.

Chao, J.L. and Hennessy, P.V. (1972). "Local scour under ocean outfall pipe-lines." *J. Water Pollution Control Federation*, 44(7), 1443-1447.

Cheng, L. (2002) "Prediction of local scour below offshore pipelines – a review," *Proc. First Conf. on Scour of Foundations*, 1, 175-183.

Chiew, Y.M. (1991). "Prediction of maximum scour depth at submarine pipelines." *J. Hydr. Engrg.*, 117(4), 452-466.

Hansen, E.A., Fredsøe, J. and Mao, Y. (1986). "Two-dimensional scour below pipelines." *Proc. Fifth Int. Symp. On Offshore Mech. and Arctic Engrg.*, ASME, New York, 3, 670-678.

Leeuwestein, W., Bijker, E.W., Peerbolte, E.B. and Wind, H.G. (1985). "The natural selfburial of submarine pipelines." *Proc 4th int. Conf. on behaviour of offshore structure*, Elsevier Science, 717-728.

Li, F. and Cheng, L. (1999) "A numerical model for local scour under pipelines," *J. Hydr. Engrg.*, 125(4), 400-406.

Li, F. and Cheng, L. (2000). "Numerical simulation of pipeline local scour with lee-wake effects," *Int. J. Offshore and Polar Engineering*, 10(3), 195-199.

Li, F. and Cheng, L. (2001). "Prediction of lee-wake scouring of pipelines in currents" *J. of Waterway, Port, Coastal, and Ocean Engineering*, 127(2), 106-112.

Lei, C., Cheng, L. and Kavanagh, K. (1999). "A finite difference solution of the shear flow over a circular cylinder." *Ocean Engineering*, 27(3), 271-290.

Liang D.F., Cheng L. and Li F. (2004). "Numerical modeling of scour below a pipeline in currents. Part II: Scour simulation." Submitted to *Coastal Engineering*, Elsevier.

Mao, Y. (1986). "The interaction between a pipeline and an erodible bed." PhD thesis, Technical University of Denmark, Lyngby, Denmark.

Sumer, B.M., Jensen, H.R. and Fredsøe, J. (1988). "Effect of lee-wake on scour below pipelines in current." *J. Of Waterway, Port, Coastal, and Ocean Engineering*, 114(5), 599-614.

van Beek, F.A. and Wind, H.G. (1990). "Numerical modelling of erosion and sedimentation around pipelines." *Coastal Engineering*, 14 107-128.

Van Rijn, L.C. (1987). "Mathematical modeling of morphological processes in the case of suspended sediment transport." *Delft Hydr. Communication No*. 382.

Wilcox, D.C. (1994). “Simulation of transition with a two-equation turbulence model.” *AIAA Journal*, 32(2), 247-255.